ANALYSIS OF HYPERSONIC FLOW OVER BLUNTED NOSE GEOMETRY FOR A DIFFERENT FINENESS RATIO AT DIFFERENT ANGLE OF ATTACK

R RAGHAVENDRA[1], SHANON ROYCE PINTO[2], JATHIN KARKERA[3], VISHWARETHA K R[4]

[1234], Mangalore Institute of Technology & Engineering, Moodabidri, 574225.
E-mail: k.vishu1994@gmail.com

AJME 2025, 23 (2); https://doi.org/10.5281/zenodo.15907719

***ABSTRACT**: This study analyses hypersonic flow over spherically blunted nose cones using CFD in ANSYS FLUENT. The focus is on fineness ratios (1.0, 3.6, and 4.7) with a constant nose radius of 2. Simulations assess static pressure, temperature, and velocity distributions at angles of 0°, 15°, and 30°. Results highlight geometric influences on flow behaviour and drag coefficients. Comparative graphs show aerodynamic impacts across configurations, emphasizing the need for drag minimization. The findings guide optimized nose cone designs for high-speed vehicles, balancing aerodynamic efficiency and thermal management under hypersonic conditions. These insights contribute to future hypersonic vehicle advancements, aiding in achieving stability and efficiency under extreme conditions.*

***KEYWORDS**: Hypersonic flow, blunted nose cone, fineness ratio, CFD simulation, aerodynamic drag*

1 INTRODUCTION

The design of hypersonic vehicles, including space shuttles and intercontinental ballistic missiles, involves significant aerodynamic challenges, especially concerning nose cone geometries. Hypersonic flows, exceeding Mach 5, create complex phenomena such as strong shock waves and significant aerodynamic heating. Among various designs, spherically blunted nose cones strike a balance between reducing drag and mitigating heating effects.

The flow field around a blunted nose cone is dominated by the interaction of incoming hypersonic flow with the geometry, forming a bow shock wave. The shock wave's shape and strength are influenced by geometric parameters such as the fineness ratio and semi-cone angle. This study examines spherically blunted nose cones with fineness ratios of 1.0, 3.6, and 4.7 at angles of attack of 0°, 15°, and 30°.

Blunt geometries increase shock standoff distance, reducing aerodynamic heating but potentially increasing drag. The angle of attack introduces further complexities by altering flow symmetry, affecting drag and lift forces. Efficiently managing these factors is crucial for enhancing vehicle performance under extreme aerodynamic loads.

This work employs CFD simulations to analyse hypersonic flow behaviour, aiming to provide insights into optimizing nose cone designs. The findings will contribute to developing more efficient high-speed vehicles with improved stability and performance across varied flight conditions.

2 METHODOLOGY

For the simulation we have chosen Ansys Fluent 2021R2 software. The solve software solves Navier Stokes Equation of the fluid flow using Finite element analysis Method through discretization (meshing). The software enables the user to define flow conditions and required functions. In our study 2D analysis of the cone is performed. The software can be reliable source for accurate results. The pre-processor and solver are very fast. We used double precision solver settings to2. The software provides workbench interface, which can enable the user put pre-processor, solver and post processor in one place making too easy to access. performed at angle of attacks 0°, 5° and 10°. The reported definitions like coefficient of lift, coefficient of drag is generated and compared.

2.1 Turbulence model

We used k-omega model for our study. The k-ω\omega turbulence model is widely used to simulate the effects of turbulent flow. It is part of the Reynolds-averaged Navier-Stokes (RANS)

family of models, where turbulence is entirely modelled rather than directly resolved. This model is called a two-equation model because, in addition to the standard conservation equations, it solves two transport equations. These equations account for the history of turbulence, including convection and diffusion effects.

2.1.1 Model

To start with the CFD process, the first step is the geometry. L/D ratio of cone geometry is made and Fluid domains around the airfoils were also created for hypersonic flow over a blunted cone for different fineness ratio at different angle of attack for the fluid flow simulation process. The type of analysis carried out is two-dimensional (2D) analysis. The geometrical dimensions of the models for numerical simulation are as follows:

a) Blunted Cone with a Fineness Ratio of 1.0 The geometry of the blunted cone has a length of 10 units and a base diameter of 10 units, with a tip diameter of 4 units. Begin by creating the cone's geometry, ensuring that the dimensions are accurately defined. Next, define the computational domain surrounding the cone. Once the geometry is complete, select the entire surface of the cone to create a surface sketch. Use the Face Split option to divide the geometry into manageable sections for further processing. Assign appropriate names to all the key surfaces, including the inlet, wall, outlet, and the blunted cone itself. This prepares the geometry for the meshing step.

(b) Blunted Cone with a Fineness Ratio of 3.6- For this case, the blunted cone has a length of 3.6 units, a base diameter of 10 units, and a tip diameter of 4 units. Start by designing the cone geometry and defining the computational domain around it. After completing the geometry, create a surface sketch by selecting the entire structure. Apply the Face Split operation to divide the geometry into distinct sections. Then, label the important surfaces, including the inlet, wall, outlet, and the blunted cone. This step ensures the geometry is ready for meshing.

(c) Blunted Cone with a Fineness Ratio of 4.6- In this case, the blunted cone has a length of 4.6 units, a base diameter of 10 units, and a tip diameter of 4 units. Start by constructing the cone geometry, carefully matching the specified dimensions, and define the surrounding computational domain. Once the geometry is complete, create a surface sketch of the entire model. Use the Face Split function to segment the geometry into appropriate sections. Assign meaningful names to all relevant surfaces, such as the inlet, wall, outlet, and the blunted cone. With this step, the geometry is prepared for meshing

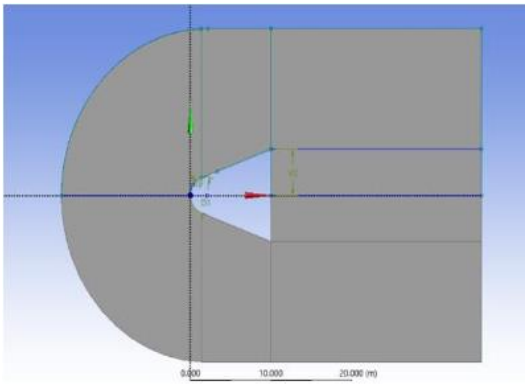

Fig. 1. Geometry of 1.0 Fineness ratio

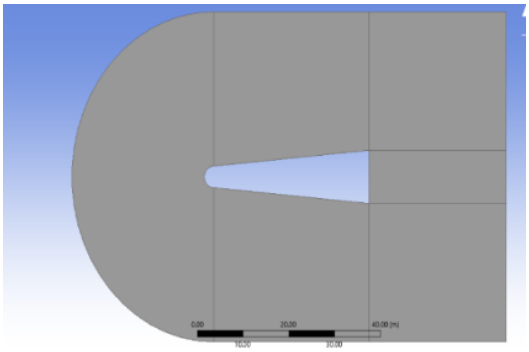

Fig. 2. Geometry of 3.6 Fineness ratio

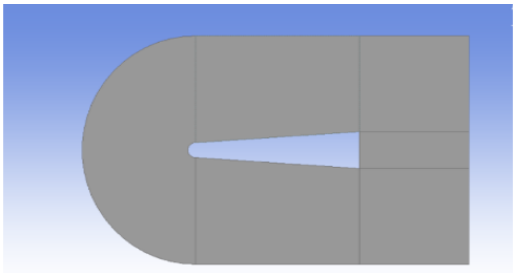

Fig. 3. Geometry of 4.6 Fineness ratio

2.2 Mesh

Structured mesh with finer layer around the blunted cone wall is generated. To obtain the structured mesh we face meshed the fluid domain faces with quadrilateral elements. The edges were sized with suitable number of divisions. It is important for the mesh around the area of blunted cone to be well structed and dense. This helps in the accuracy of the results that are generated. After face mesh we used size meshing set to no of divisions 200. To set the boundaries for the fluid flow, we have to create named selections. The named selections created are inlet, outlet, farfield.

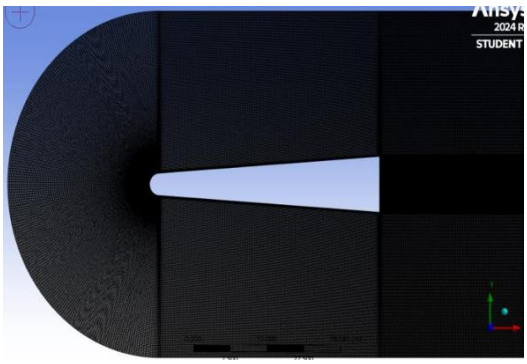

Fig. 4. Fine Mesh around the blunted cone

2.3 Solver/setup

The density-based solver at a steady state was used in this project. The turbulence model used is k omega, with energy equation on. The material used was fluid select air in it with ideal gas density and choose viscosity Sutherland law. Under boundary conditions select inlet gauge pressure 10 with Mach 8.X-component and Y-component flow direction to change the angle of attack. Thermal temperature is 288k the pressure at the outlet is 0 pa with no slip condition is applied to the blunted wall.

Table 1. This table illustrates the mesh statistics

Nodes	elements
245222	244012

Table 2. Boundary conditions assigned to the named selections

Name selection	Boundary condition
Inlet	Pressure far field
Wall	Pressure far field
Outlet	Pressure outlet
Blunted nose cone	Wall

3 RESULTS AND DISCUSSION

3.1 Figures and table

3.1.1 Velocity contour

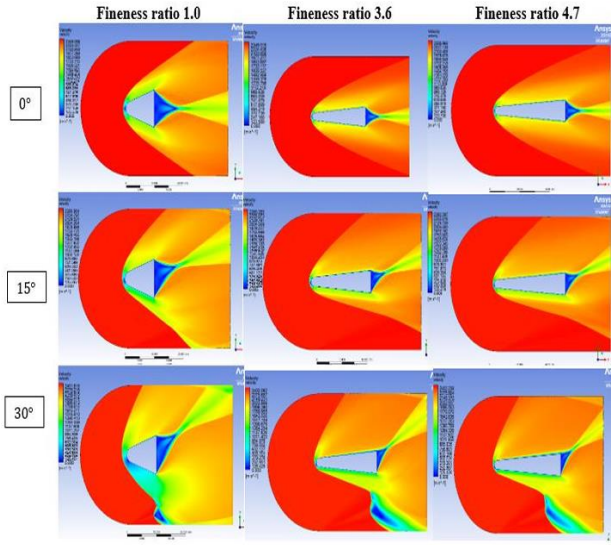

Fig. 5. Velocity Contour for fineness ratio 1.0,3.6 and 4.7 at angles of attack 0°, 15° and 30°

In the above figure-5, the velocity contours of Mach number 8, for fineness ratio 1.0,3.6 and 4.7 at angles of attack 0°, 15° and 30°. In all the three geometries, there is a visible layer of least Mach number(blue) around the profile and for higher Mach number denoted (red) around the profile. Fineness ratio of 1.0

- 0° AOA: Velocity decreases from 2420 m/s at the tip to 1730 m/s downstream, with significant drag due to the large stagnation region.
- 15° AOA: Velocity ranges from 1070 m/s (stagnation point) to 2290 m/s downstream, causing flow asymmetry, pressure variations, and flow separation.
- 30° AOA: Velocity peaks at 2402 m/s on the flow side but drops to 780 m/s in the recirculation zone, resulting in high drag and wake turbulence.

Fineness ratio of 3.6, Represents a moderately streamlined geometry that improves aerodynamic performance.

- At 0° AOA: The flow is symmetric, with maximum velocity (~2348 m/s) occurring near the tip due to acceleration. A normal shock forms at the leading edge, and low-velocity regions are confined near the geometry's surface.
- At 30° AOA: The flow becomes asymmetric, with higher velocities (~2380 m/s) on the side experiencing compression. The shock wave shifts asymmetrically, and larger low-velocity zones appear near the stagnation region on the lower surface.
- At 30° AOA: when the free-stream flow (~2402 m/s) hits the wedge at a 30° angle

- of attack, forming an oblique shock that reduces velocity to ~1000–1500 m/s. A stagnation region (~0–126 m/s) forms at the leading edge, while flow accelerates along the surface before shock interaction.

Fineness ratio of 4.7, with its highly streamlined shape, achieves the best aerodynamic performance.

- At 0° AOA, the velocity decreases from 2350 m/s at the tip to 1230 m/s downstream, indicating significant drag due to the stagnation zone. Symmetrical flow with a pronounced shockwave near the nose.
- At 15° AOA, the velocity ranges from 2380 m/s downstream to as low as 125 m/s at the stagnation point, highlighting flow asymmetry. Increased pressure variations and localized flow separation on the leeward side of the nose.
- At 30° AOA: The velocity contour shows a high-speed region near the nose tip, with velocities reaching up to 2350 m/s, driven by the high-Mach flow and the nose's converging shape. A velocity gradient forms along the surface, decreasing away from the tip. Near the stagnation point, the velocity drops significantly, creating a low-speed, high-pressure zone with recirculation.

3.1.2 Temperature contour

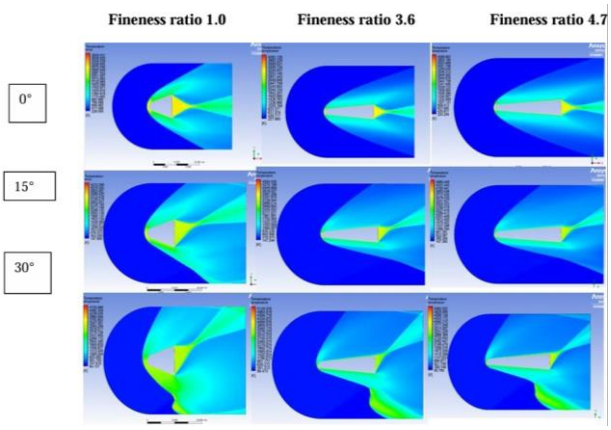

Fig. 6. Temperature contour for fineness ratio 1.0,3.6 and 4.7 at angles of attack 0°, 15° and 30°

In the above figure 7, For the Fineness ratio (L/D = 1.0), very high heating takes place at the front of stagnation point.

- At 0° AOA, at front temperature reaches to 3431 K, and it cools down to 228 K further back.
- At 15° AOA, the cone side where airflow comes in contact gets hotter, up to 3955 K, while the 0° 15° 30°.
- At 30° AOA, the windward side heats up even more, reaching 4569 K, while the leeward side remains cooler because of air separation.

Fineness ratio (L/D = 3.6) which is moderately streamlined shaped heating is less intense.

- At 0° AOA, the front reaches 2930 K, with a smooth drop in the temperature further back. At 15° AOA, the windward side heats to 3450 K, but the leeward side remains cooler, lowering stresses on the surface.
- At 30° AOA, the windward side reaches 4320 K, but overall heating is less than with the blunt shape.

Fineness ratio (L/D = 4.7), which is most streamlined shape were heat is highest due to the sharper design.

- At 0° AOA, the front reaches 5129 K.
- At 15° AOA, the windward side heats up to 5500 K, while the leeward side stays cooler.
- At 30° AOA, the windward side reaches at 6000 K, with large differences in heating between the sides. Sharper shapes handle airflow better but need stronger heat protection because of higher front and windward temperatures.

3.1.3 pressure contour

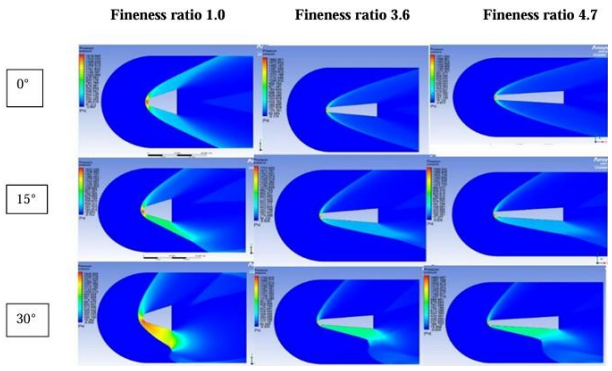

Fig. 7. Pressure Contour for fineness ratio 1.0,3.6 and 4.7 at angles of attack 0°, 15° and 30°

In the above figure 6 for the Fineness Ratio (L/D = 1.0), the pressure at the stagnation point reaches 1571 kPa at 0° AOA, with a symmetric decrease downstream to 350–400 kPa.

- At 15° AOA, asymmetry appears, with peak pressure reaching 1569 kPa on the windward side and much lower on the leeward side.
- At 30° AOA, the windward side experiences the highest pressure of 1680

- kPa, while the leeward side faces lower pressure due to increased flow separation.

Fineness Ratio (L/D = 3.6), stagnation pressure peaks at 1450 kPa at 0° AOA, with a smooth pressure drop along the surface.

- At 15° AOA, windward pressure rises to 1500 kPa, while the leeward side shows lower but more balanced values compared to the 1.0 ratio.
- At 30° AOA, windward pressure reaches to 1650 kPa, with better pressure handling and less flow separation than the other blunt geometry.

Fineness Ratio (L/D = 4.7) we can see stagnation pressures of 1700 kPa at 0° AOA, with efficient distribution and minimal drag.

- At 15° AOA, windward pressures rise to 1750 kPa with sharper gradients, while the leeward side maintains lower values.
- At 30° AOA, windward pressure peaks at 1800 kPa, the highest among all ratios that we have considered with notable asymmetry
- and strong aerodynamic forces due to the flow compression.

3.1.3 Tables

Table 3. 1.0 Fineness ratio drag and drag % at different AOA

SI NO	AOA α (°)	DRAG(N)	DRAG %
1	0	5499	0
2	15	5737	4.33
3	30	6630	20.56

Table 4. 3.6 Fineness ratio drag and drag % at different AOA

SI NO	AOA α (°)	DRAG(N)	DRAG %
1	0	6804	0
2	15	7343	7.92
3	30	8306	22.6

Table 5. 4.6 Fineness ratio drag and drag % at different AOA

SI NO	AOA α (°)	DRAG(N)	DRAG %
1	0	5392	0
2	15	5622	4.27
3	30	6455	19.74

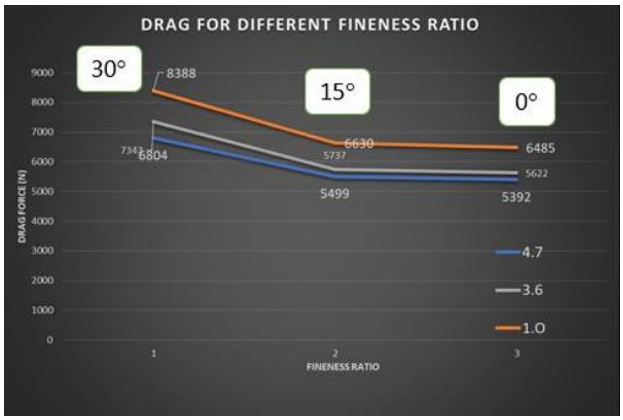

Fig. 8. Drag vs Different (1.0,3.6,4.7) Fineness ratio for 0°,15°,30°Angle of Attack

In the above graph-1 shows that drag force decreases with an increase in fineness ratio for all angles of attack (0°, 15°, and 30°), indicating that slender bodies experience less drags than blunt ones. Drag increases with angle of attack, with 30° showing the highest values across all fineness ratios. At fineness ratio 1.0, drag is highest (~7348 N at 0° to ~8388 N at 30°). For fineness ratios 3.6 and 4.7, drag reduces significantly (~5499 N and ~5392 N at 0°, respectively). Slender bodies (higher fineness ratios) are also less sensitive to changes in AOA, making them more aerodynamically efficient

Table 6. 1.0,3.6 & 4.6 Fineness ratio drag and drag % at different AOA.

Angle of Attack α (°)	Drag (Fineness Ratio 1.0)	Drag (Fineness Ratio 3.6)	Drag (Fineness Ratio 4.6)	Drag % (Relative to 3.6)	Drag %(Relative to 4.6)	Error % (Relative to 3.6)	Error % (Relative to 4.6)
0	6804	5499	5392	23.73	26.19	19.18	20.75
15	7343	5737	5622	27.99	30.61	21.87	23.44
30	8305	6630	6455	25.26	28.66	20.1	22.28

The table summarizes drag data for a hypersonic vehicle at three fineness ratios (1.0, 3.6, and 4.7) across angles of attack (0°, 15°, and 30°). Drag decreases as the fineness ratio increases, with the 4.7 ratio consistently showing the lowest drag. At 0°, the drag for a fineness ratio of 1.0 is 23.73% and 26.19% higher than for 3.6 and 4.7, respectively, with similar trends observed at 15° and 30°. The drag percentage differences and error percentages highlight the variations and deviations relative to 3.6 and 4.7. Overall, increasing the fineness ratio significantly reduces drag, with the effect becoming more pronounced at higher angles of attack.

4 CONCLUDING REMARKS

Drag increases with AOA due to the asymmetry in the flow field, which effectively due to its frontal area. At 15°, drag increases moderately, with percentage increasing ranging from 4.27% to 7.92% across the fineness ratios. At 30°, the drag increases more significantly, with percentage increments between 19.74% and 22.6%. When comparing the relative performance of the fineness ratios, the 3.6 and 4.7 fineness ratios achieve substantial drag reductions relative to the 1.0 ratio at all angles of attack. When comparing the relative performance of the fineness ratios, the 3.6 and 4.7 fineness ratios achieve substantial drag reductions relative to the 1.0 ratio at all angles of attack. For instance, at 0°, the 3.6 and 4.7 ratios achieve drag reductions of 23.73% and 26.19%, respectively, relative to the 1.0 ratio. The 4.7 fineness ratio is the most efficient geometry in terms of the drag reduction, making it a favorable choice for the design of hypersonic vehicles.

5 REFERENCES

Narayanan Subramanian, Rakesh Kumar, Chintoo Sudhiesh Kumar, et al. (2020). "Hypersonic flow past a spherically blunted nose cone: A computational study." “Journal of AIP”, 2204, 020002.

Ashish Narayan, S. Narayanan, Rakesh Kumar (2017). "Hypersonic flow past nose cones of different geometries." “International Journal of Engineering Research and Technology”, 6(5), 694 698.

Savino, R., & Paterna, D. (2004). Blunted cone–flare in hypersonic flow. “Journal of Spacecraft and Rockets”, 41(5), 733–739.

Paredes, P., Scholten, A., Choudhari, et al. (2004). Combined bluntness and roughness effects on cones at hypersonic speeds. “AIAA Journal”, 42(3), 415–423.

Watanabe, Y., Suzuki, K., & Rathakrishnan, E. (2022). Aerodynamic characteristics of breathing blunt nose configuration at hypersonic speeds. “Journal of Aerospace Science and Technology”, 130(2), 107-152.

Zhijun, Z., Wang, X., & Tianyi, L. (2019). Hypersonic nonequilibrium flow simulations of a hemispherical nose with a counterflowing jet. “Journal of Acta Astronautica”, 165(1), 123–132.

Zhu, L., Li, Y., Chen, X., Li, H., Li, W., & Li, C. (2019). Hypersonic flow characteristics and relevant structure thermal response induced by the novel combined spike-aerodome and lateral jet strategy. “Journal of Spacecraft and Rockets”, 56(3), 654–663.

Holden, M. S., Rodriguez, K. M., & Nowak, R. J. (1991). Studies of shock/shock interaction on smooth and transpiration-cooled hemispherical nose tips in hypersonic flow. “Journal of NASA Langley Technical Reports”, 19(1),156-220.

Santos, W. F. N. (2003). Aerodynamic heating on blunt nose shapes in rarefied hypersonic flow. “Journal of Thermophysics and Heat Transfer”, 17(2), 232–240.

Feldhuhn, R. H., & Pasiuk, L. (1968). An experimental investigation of the aerodynamic characteristics of slender hypersonic vehicles at high angles of attack. “Journal of NASA Technical Note”, D-4890.

Yadav,R.,&Guven, U. (2013).Aerothermodynamics of a hypersonic vehicle with a forward-facing parabolic cavity at nose. “Journal of Aerospace Engineering”, 26(1), 124–132.

King, H. H., & Talbot, L. (1964). Effect of mass injection on the drag of a slender cone in hypersonic flow. “AIAA Journal”, 2(6), 1052–1058.

Sudarshan, B., Jagadeesh, G., & Saravanan, S. (2021). Experimental investigation on aerothermal effects of forward-facing cylindrical and parabolic cavity in hypersonic flow. “Journal of Aerospace Science and Technology”, 112(1), 106598.

Marley, C. D., & Riggins, D. W. (2011). Numerical study of novel drag reduction techniques for hypersonic blunt bodies. “Journal of Spacecraft and Rockets”, 48(4), 637–649.

Fayazbakhsh, M. A., & Barzegar Gerdroodbary, S. M. (2011). Numerical study on heat reduction of various counterflowing jets over highly blunt cone in hypersonic flow. “International Journal of Hyper Sonic’s”, 2(1), 45–53. notation